ANALYSIS OF ELECTROMAGNETIC FIELD DISTRIBUTIONS IN A 915 MHz SINGLE-MODE MICROWAVE APPLICATOR

G. Q. Xie

Institute for Materials Research
Tohoku University
Sendai 980-8577, Japan

M. Suzuki

National Institute for Fusion Science
Orosi-cho, Toki 509-5292, Japan

D. V. Louzguine-Luzgin and S. Li [†]

WPI Advanced Institute for Materials Research
Tohoku University
Sendai 980-8577, Japan

M. Tanaka and M. Sato

National Institute for Fusion Science
Orosi-cho, Toki 509-5292, Japan

A. Inoue [‡]

WPI Advanced Institute for Materials Research
Tohoku University
Sendai 980-8577, Japan

Corresponding author: G. Q. Xie (xiegq@imr.tohoku.ac.jp).

[†] D. V. Louzguine-Luzgin is also with Institute for Materials Research, Tohoku University, Sendai 980-8577, Japan

[‡] A. Inoue is also with Institute for Materials Research, Tohoku University, Sendai 980-8577, Japan

Abstract—The electromagnetic field distributions in the waveguide of a 915 MHz single-mode microwave sintering applicator equipped with a loading pressure system were simulated using a JMAG-Studio program. The disturbance in the magnetic field as well as in electric field was caused by the insertion of the alumina loading pressure system due to reflection effect of alumina. However, the separated magnetic field and electric field maxima can be obtained by adjusting position of the alumina loading pressure system in the waveguide. The simulation results were evaluated by comparison with experimental measurement.

1. INTRODUCTION

Microwave-induced heating and sintering process has attracted increasing attention due to its significant advantages in material processing compared to conventional processes. Microwaves allow volumetric heating of materials. Microwave energy transforms into heat inside the material, which results in significant energy savings and reduction in process time [1]. Microwave energy could be used for processing full-scale ceramic products [2, 3], polymers [4] and in rubber industry [5]. However, applicability of microwave sintering to metals was ignored due to the fact that they reflect microwaves. Roy et al. reported that powdered metals could be heated rapidly by microwaves and fully sintered samples were obtained in a multimode cavity [6, 7]. Subsequently, microwave heating of the powdered metals in separated electric (E-) field and magnetic (H-) field was performed in a single mode applicator [8–10]. The microwave sintering of various metallic powders, steels and non-ferrous alloys produced sintered samples within tens of minutes at sintering temperatures between 1370 K to 1570 K [11–13].

Recently, we attempted to consolidate Ni-based metallic glass alloy powders and its mixed powders blended with crystalline particulates by the microwave-induced heating and sintering process [14–17]. It was shown that heating was more efficient in a magnetic field. The sintered compacts retained the glassy structure. However, powder particles in the sintered compacts were very weakly bonded and the compacts obtained had quite a low relative density. In order to increase density of the sintered samples and improve sintering behavior of the metallic glass alloy powders, we have built a new 915 MHz, 5 kW single-mode microwave sintering applicator with separated electric (E-) field and magnetic (H-) field, equipped with a loading pressure system. In the present study, we simulated the electromagnetic field distributions in the waveguide for this 915 MHz single-mode microwave sintering

applicator based on a finite element method using a JMAG-Studio program. The distributions of the electric field and magnetic field at various conditions, such as the positions of the sample and alumina loading pressure system, the properties of the loading pressure system materials, and so on, were investigated. The simulation results obtained were evaluated by comparing with the experimental results.

2. SIMULATION METHOD

In this study, a 915 MHz single-mode microwave sintering applicator equipped with loading pressure system was used for simulation. Figure 1 shows a schematic illustration of the microwave applicator. In this system, a movable plunger is set at the end of the wave-guide, which acts as a metal wall, and the wave is reflected.
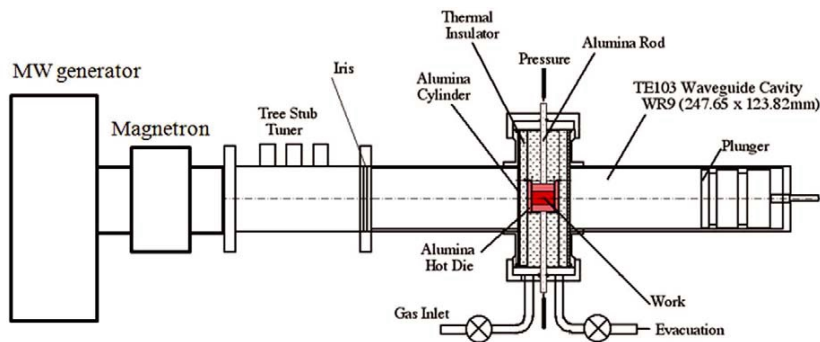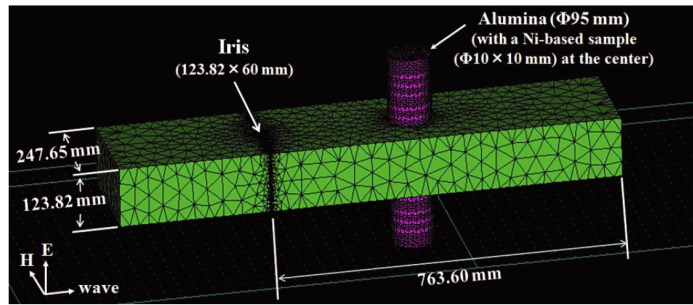

Figure 1. Schematic illustration of the microwave sintering applicator equipped with loading pressure system.

The simulation of the electromagnetic field distributions is based on the finite element method (FEM) using a JMAG-Studio program. Figure 2 shows the schematic finite element model and initial mesh. Alumina (Al_2O_3) was used as the mould material in the loading pressure system. The sintered sample is the Ni-based metallic glassy alloy powders. The stainless steel was used as the metal wall of the waveguide cavity. The detailed dimensions of the waveguide cavity and the practical design parameters of the alumina loading pressure unit and the sintered samples are also given in Figure 2. Some material property parameters used in the simulations are shown in Table 1.

Table 1. Some material property parameters used in the simulations.

|	Air	Alumina	Ni	Fe
Relative permittivity (ε')	1	9	31	1
Relative permittivity (ε'')	0	0	0	0
Conductivity, σ, $[(\Omega \cdot m)^{-1}]$	—	—	1.45×10^7	1.03×10^7
Relative permeability (μ')	1	7.9×10^{-4}	600	5000
Relative permeability (μ'')	0	0	—	—

Figure 2. Finite element mesh for electromagnetic field simulations in the computational software, JMAG-Studio. The indicated data are practical design parameters.

3. RESULTS AND DISCUSSION

### 3.1. Simulation of Electromagnetic Field Distributions

The simulation of the electromagnetic field distributions was carried out using the JMAG-Studio program for some practical working conditions in the 915 MHz single-mode microwave sintering applicator. Figure 3 shows the calculated distributions of the magnetic field (Figure 3(a)) and electric field (Figure 3(b)) in the waveguide for a case without any insertion (namely without the loading pressure system

as well as without the samples), the right hand side is the plunger (metal wall). It is seen that there are four peaks in the magnetic field as well as in the electric field at the distance from iris to the plunger. Considering the two distributions and their symmetries, it is pointed out that there are four specific positions with respect to the magnetic-field and electric-field conditions, as indicated in Figure 3(c). Yoshikawa et al., [9, 18] has compared the heating behavior by placing a specimen in either position.
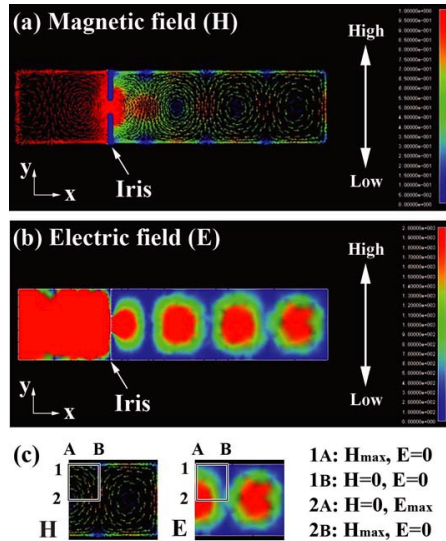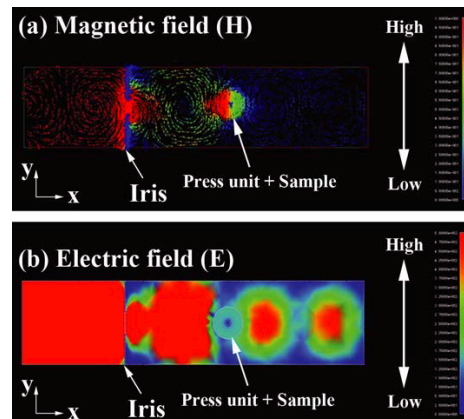

Figure 3. Simulated distributions of the magnetic field (a) and electric field (b) in the wave guide for a case without the loading pressure system and samples. (c) Four specific positions are indicated with respect to the magnetic field and electric field.

It is of importance to understand how the distributions are distorted by existence of the specimens and the loading pressure system. Figure 4 shows the magnetic field (Figure 4(a)) and electric field (Figure 4(b)) distributions in the wave guide for a case of insertion with a Ni-based sample. The sample of 10 mm in diameter and 10 mm in length is placed in the single mode applicator at a distance of 328 mm away from iris. In comparison with those without insertion (Figure 3), it is shown that no obvious alteration in the electromagnetic field distributions and in the intensity is induced. Figure 5 shows a simulation result of the magnetic field (Figure 5(a)) and electric field (Figure 5(b)) distributions in the wave guide for a case of insertion with an alumina loading pressure unit added with the Ni-based sample in
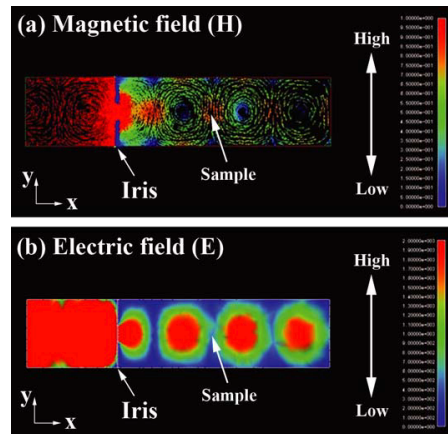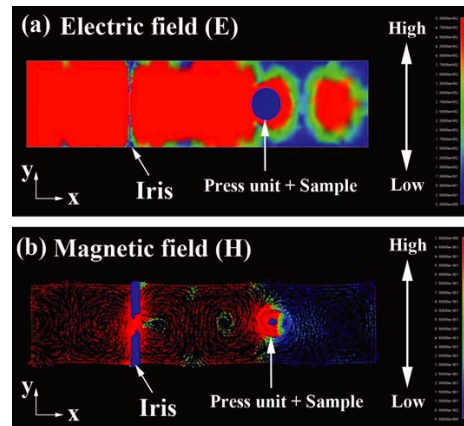
Figure 4. Simulated distributions of the magnetic field (a) and electric field (b) in the wave guide for a case of insertion with a Ni-based sample.

Figure 5. Simulated distributions of the magnetic field (a) and electric field (b) in the wave guide for a case of insertion with an alumina loading pressure system added with a Ni-based sample in the center. The size of the loading pressure system is 95 mm in diameter, and the size of the Ni-based sample is 10 mm in diameter and 10 mm in length. They are placed in the microwave applicator with a distance of 328 mm away from iris.

the center. The alumina loading pressure system of 95 mm in diameter is placed in the single mode applicator at the distance of 328 mm away from iris. The results indicate that obvious alterations in the electromagnetic field distributions and in the intensity are caused by insertion of the alumina loading pressure system, while the effect of changing height of the alumina loading pressure system is very little. In view of the simulation results, it is clear that there are a magnetic field maximum and an electric field minimum at 328 mm away from the iris in the 915 MHz single-mode microwave sintering applicator. Thus, we can place the specimens in this area in the applicator, examine the microwave heating behavior of various materials and study the effect of the independent magnetic field on heating of the materials.

Based on the above simulated results, if the position of the inserted alumina loading pressure unit moves backward a distance of 0.5λ (namely moves to the position of 437 mm away from iris), it should be in a position with an electric field maximum. Figure 6 shows the simulation results of the electric field and magnetic field distributions in the wave guide with the insertion of an alumina loading pressure system containing a Ni-based sample. It is seen that there is an electric field maximum at this position of 437 mm away from the iris diaphragm, as shown in Figure 6(a). However, it is also observed that there is certain magnetic field distribution in the sample position (Figure 6(b)).
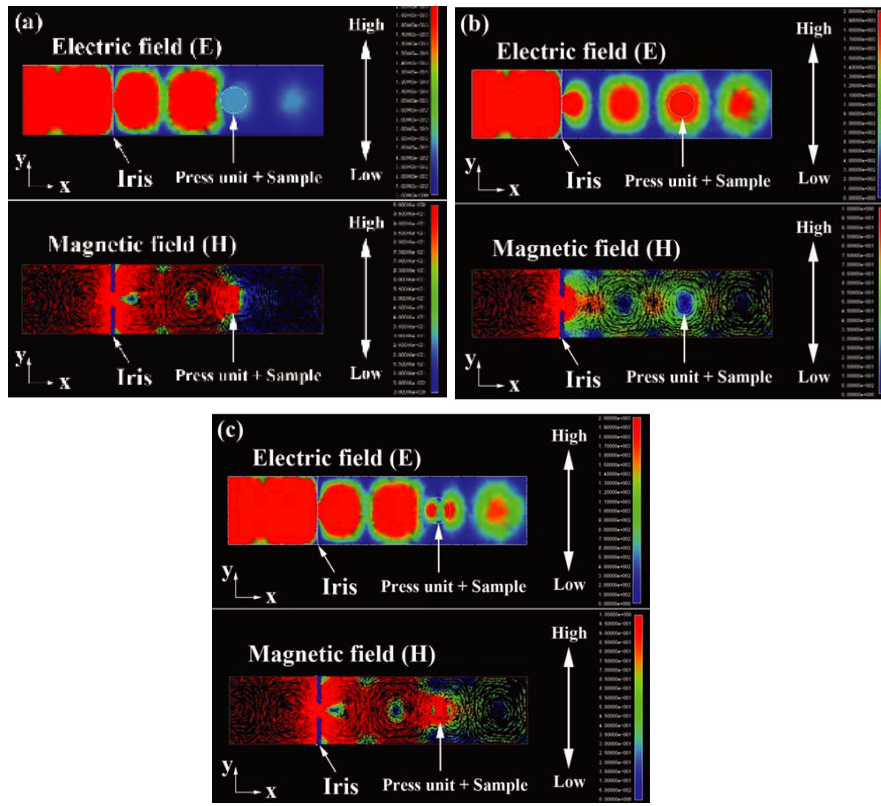

Figure 6. Simulation distributions of the electric field (a) and magnetic field (b) in the wave guide for a case of insertion with an alumina loading pressure system added with a Ni-based sample in the center. The insertion with the same size as those of Figure 5 is placed in the microwave applicator with a distance of 437 mm away from iris.

In order to clarify the reason of the magnetic field distribution, some potential influence factors were considered and the corresponding simulations were carried out. At the first, we simulated the cases of insertion with only a Ni-based sample or only an alumina loading pressure unit at the position of 437 mm away from the iris diaphragm. In the case of inserting Ni-based sample only, the electric field and magnetic field distributions and their intensities were similar to those observed without any insertion (Figure 3). No obvious alteration was caused by the insertion of the Ni-based sample. In the case of insertion with only an alumina loading pressure unit, the similar characteristic features in the field distribution and in the intensity were achieved as those obtained on inserting an alumina loading pressure system containing a Ni-based sample (Figure 6). The disturbance was caused not only in the electric field but also in the magnetic field by the insertion of the alumina loading pressure unit. This is because the alumina is a proto-typical ceramic material with excellent dielectric properties. This material has a very low dielectric loss at room temperature [19]. The disturbance is caused by modifying the resonance mode which originates from the dielectric polarization by insertion of the alumina dielectric material into the electromagnetic wave. The alumina acts as a reflected boundary.

We also investigated the effect of the physical properties of the loading pressure unit materials on the electric field and magnetic field distributions. Figure 7 shows the simulation results of the electric field and magnetic field distributions in the wave guide with insertion of a loading pressure unit containing a Ni-based sample at a distance of 437 mm away from the iris diaphragm for three kinds of loading pressure system materials. It is demonstrated that the disturbance in the electric field and magnetic field distributions occurs in the case of the loading pressure unit material with a relative permittivity (ε') >1 due to the electromagnetic wave reflection by the mould material, while the effect is very little for the case of $\varepsilon' = 1$.

Based on the above simulation results, it is demonstrated that the separated electric field and magnetic field maxima can be obtained by adjusting the position of the alumina loading pressure system in this 915 MHz single-mode microwave sintering applicator. It is possible to determine the position with an electric field maximum and a magnetic field minimum by modifying the loading pressure unit material or fine adjusting the position of the loading pressure unit in the microwave applicator.

Figure 7. Simulated distributions of the electric field and magnetic field in the wave guide with insertion of a loading pressure system added with a Ni-based sample at a distance of 437 mm away from iris for three kinds of loading pressure unit materials: (a) with a relative permeability $(\mu') = 7.9 \times 10^{-4}$, and a relative permittivity $(\varepsilon') = 9$; (b) $\mu' = 7.9 \times 10^{-4}$, $\varepsilon' = 1$; (c) $\mu' = 1$, $\varepsilon' = 9$.

## 3.2. Comparison with Experimental Measurements

In order to evaluate the reliability of the simulation results, we measured the magnetic field and electric field distributions in the waveguide for the 915 MHz single-mode microwave sintering applicator. Figure 8(a) shows a schematic illustration of the experimental measurement. Figure 8(b) presents a measured result of the magnetic field distribution in the wave guide for the case without the loading pressure unit and sample which is same as the case in Figure 3. Figure 8(c) shows a measured magnetic field distribution in the wave

(a)

(b)

(c)
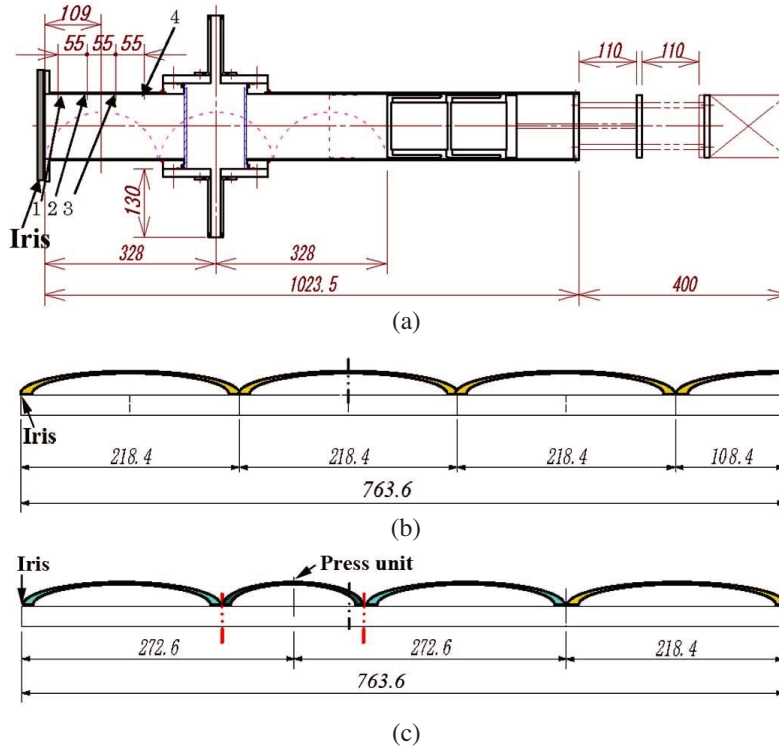
Figure 8. (a) Schematic diagram of the experimental measurement: Points 1 to 4 are the measured position. (b) The measured magnetic field distribution in the wave guide for the case without the loading pressure system and sample. (c) The measured magnetic field distribution in the wave guide for the case with insertion of an alumina loading pressure system containing a Ni-based sample in the center with the same size and position as those in Figure 5.

guide for the case with insertion of an alumina loading pressure unit containing a Ni-based sample in the center with the same size and position as those in Figure 5. By comparing Figure 8(b) with Figure 3(a) as well as Figure 8(c) with Figure 5(a), it is demonstrated that the results of the experimental measurement are similar to those of simulation.

Figure 9 shows the photograph of our custom-made 915 MHz single-mode microwave sintering applicator which contains the separated magnetic field unit and electric field unit, and equipped with the alumina loading pressure systems. Utilizing this microwave
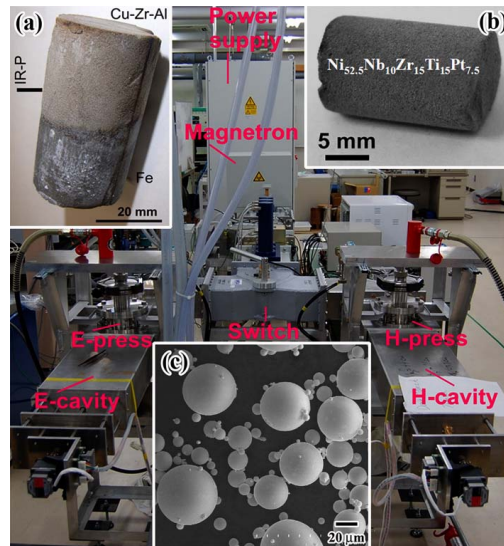
Figure 9. Photograph of the 915 MHz single-mode microwave sintering applicator with the separated magnetic field and electric field, and combined with the vacuumed alumina loading pressure systems. The inserts (a, b) are optical micrographs of some obtained samples using this applicator in magnetic field maximum: (a) a two-phase $Cu_{50}Zr_{45}Al_5$ glassy-Fe crystal sample [20], (b) a sintered $Ni_{52.5}Nb_{10}Zr_{15}Ti_{15}Pt_{7.5}$ glassy sample, and (c) a scanning electron microscopy image of the gas-atomized $Ni_{52.5}Nb_{10}Zr_{15}Ti_{15}Pt_{7.5}$ glassy alloy powders before the microwave sintering with a particle size below $63\,\mu m$.

applicator, we sintered a number of samples of various materials. The inserts in Figure 9 show some examples of the obtained bulk metallic glass and composite samples sintered in the magnetic field maximum area under a low applied pressure of 5 MPa. The sintered bulk samples with above 70% relative density have been produced.

4. CONCLUSIONS

Based on the finite element method using a JMAG-Studio program, we have simulated the electric field and magnetic field distributions in the waveguide for a 915 MHz single-mode microwave sintering applicator equipped with the loading pressure system. The results indicated that the disturbance was caused in the magnetic field as well as in electric

field by the insertion of the alumina loading pressure system due to reflection effect of alumina. The separated magnetic field and electric field maxima can be obtained by adjusting the position of the alumina loading pressure system in the waveguide. The simulation results have been demonstrated by experimental measurements. The simulation results might provide an important basis for adjusting the insertion position and understanding the electric field and magnetic field distributions in the waveguide for the microwave sintering applicator.

ACKNOWLEDGMENT

REFERENCES

1. Bykov, Y. V., K. I. Rybakov, and V. E. Semenov, "High-temperature microwave processing of materials," *J. Phys. D: Appl. Phys.*, Vol. 34, R55–R75, 2001.
2. Clark, D. and W. H. Sutton, "Microwave processing of materials," *Annu. Rev. Mater. Sci.*, Vol. 26, 299–331, 1996.
3. Katz, J. D., "Microwave sintering of ceramics," *Annu. Rev. Mater. Sci.*, Vol. 22, 153–170, 1992.
4. Akyel, C. and E. Bilgen, "Microwave and radio-frequency curing of polymers: Energy requirements, cost and market penetration," *Energy*, Vol. 14, No. 12, 839–851, 1989.
5. Chabinsky, I. J., "Practical applications of microwave energy in the rubber industry," *Elastomerics*, Vol. 115, No. 1, 17–20, 1983.
6. Roy, R., D. Agrawal, J. P. Cheng, and S. Gedevanishvili, "Full sintering of powdered-metal bodies in a microwave field," *Nature*, Vol. 399, 668–670, 1999.
7. Anklekar, R. M., K. Bauer, D. Agrawal, and R. Roy, "Improved mechanical properties and microstructural development of microwave sintered copper and nickel steel PM parts," *Powder Metall.*, Vol. 48, No. 1, 39–46, 2005.

8. Roy, R., R. Peelamedu, L. Hurtt, J. P. Cheng, and D. Agrawal, "Definitive experimental evidence for microwave effects: Radically new effects of separated E and H fields, such as decrystallization of oxides in seconds," *Mater. Res. Innovat.*, Vol. 6, No. 3, 128–140, 2002.

9. Yoshikawa, N., E. Ishizuka, and S. Taniguchi, "Heating of metal particles in a single-mode microwave applicator," *Mater. Trans.*, Vol. 48, No. 3, 898–902, 2006.

10. Buchelnikov, V. D., D. V. Louzguine-Luzgin, G. Q. Xie, S. Li, N. Yoshikawa, M. Sato, A. P. Anzulevich, I. V. Bychkov, and A. Inoue, "Heating of metallic powders by microwaves: Experiment and theory," *J. Appl. Phys.*, Vol. 104, 113505, 2008.

11. Anklekar, R. M., D. Agrawal, and R. Roy, "Microwave sintering and mechanical properties of PM copper steel," *Powder Metall.*, Vol. 44, No. 4, 355–362, 2001.

12. Rybakov, K. I., V. E. Semenov, S. V. Egorov, A. G. Eremeev, I. V. Plotnikov, and Y. V. Bykov, "Microwave heating of conductive powder materials," *J. Appl. Phys.*, Vol. 99, 023506, 2006.

13. Upadhyaya, A., S. K. Tiwari, and P. Mishra, "Microwave sintering of W-Ni-Fe alloy," *Scripta Mater.*, Vol. 56, No. 1, 5–8, 2007.

14. Yoshikawa, N., D. V. Louzguine-Luzgin, K. Mashiko, G. Q. Xie, M. Sato, A. Inoue, and S. Taniguchi, "Microstructural changes during microwave heating of $Ni_{52.5}Zr_{15}Nb_{10}Ti_{15}Pt_{7.5}$ metal glasses," *Mater. Trans.*, Vol. 48, No. 3, 632–634, 2007.

15. Xie, G. Q., S. Li, D. V. Louzguine-Luzgin, Z. P. Cao, N. Yoshikawa, M. Sato, and A. Inoue, "Effect of Sn on microwave-induced heating and sintering of Ni-based metallic glassy alloy powders," *Intermetallics*, doi:10.1016/j.internet.2008.08 016.

16. Li, S., G. Q. Xie, D. V. Louzguine-Luzgin, Z. P. Cao, N. Yoshikawa, M. Sato, and A. Inoue, "Microwave sintering of Ni-based bulk metallic glass matrix composite in a single-mode applicator," *Mater. Trans.*, Vol. 49, No. 12, 2850–2853, 2008.

17. Xie, G. Q., S. Li, D. V. Louzguine-Luzgin, Z. P. Cao, N. Yoshikawa, M. Sato, and A. Inoue, "Microwave-induced sintering of NiNbTiPt metallic glass blended with Sn powders using a single-mode applicator," *J. Phys.: Conference Series*, 2009 [in press].

18. Cheng, J. P., R. Roy, and D. Agrawal, "Experimental proof of major role of magnetic field losses in microwave heating of metal and metallic composites," *J. Mater. Sci. Lett.*, Vol. 20, No. 17, 1561–1563, 2001.

19. Breeze, J. D., X. Aupi, and N. M. Alford, "Ultralow loss polycrystalline alumina," *Appl. Phys. Lett.*, Vol. 81, No. 26, 5021–5023, 2002.

20. Louzguine-Luzgin, D. V., G. Q. Xie, S. Li, A. Inoue, N. Yoshikawa, and M. Sato, "Microwave-induced heating of a single glassy phase and a two-phase material consisting of a metallic glass and Fe powder," *Phil. Mag. Lett.*, 2009 [in press].